

Physical Properties of s_{\pm} Superconductors as a Model of Iron Pnictides

Alexander Golubov

University of Twente, The Netherlands

In collaboration with

A. Brinkman, University of Twente,
Netherlands

O.V. Dolgov, Max Planck Institute, Stuttgart,
Germany

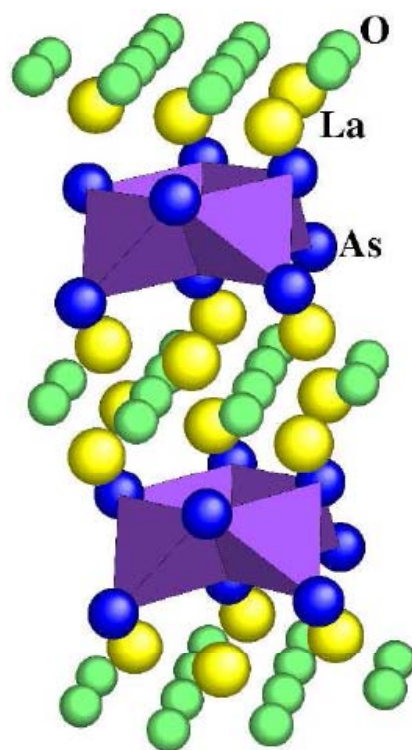
I.I. Mazin, D. Parker, Naval Research Lab,
Washington, USA

Y. Tanaka, Nagoya University, Japan

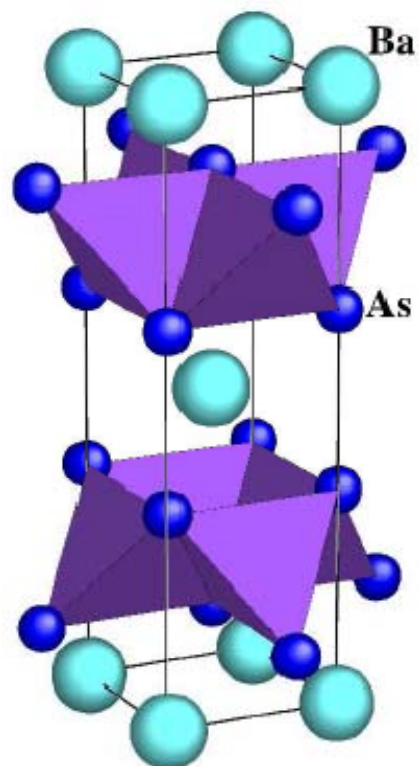
Outline

- Introduction.
- Robustness of \mathbf{s}_{\pm} pairing against impurities.
- Absence of the *Hebel-Slichter* peak in NMR relaxation and T -dependence of $1/T_1$.
- Gaps and electromagnetic response in the \mathbf{s}_{\pm} model
- Tunneling in the \mathbf{s}_{\pm} model

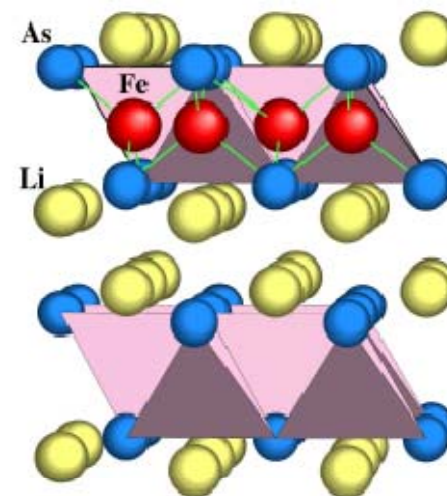
Crystal structure of FeAs superconductors



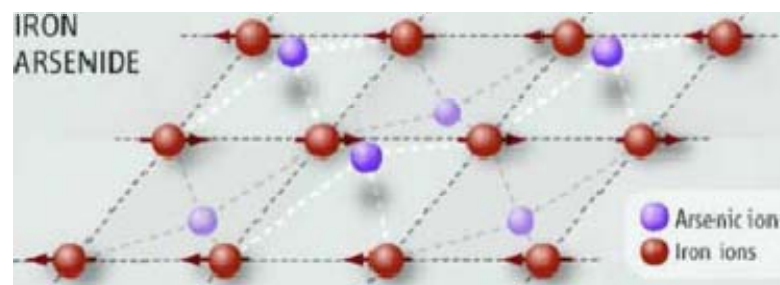
LaOFeAs



BaFe₂As₂



LiFeAs



FeAs tetrahedra form two-dimensional layers surrounded by LaO, Ba or Li.
Fe ions inside tetrahedra form a square lattice.

Basic Experiments on FeAs

J|A|C|S
COMMUNICATIONS

Published on Web 02/23/2008

February 2008

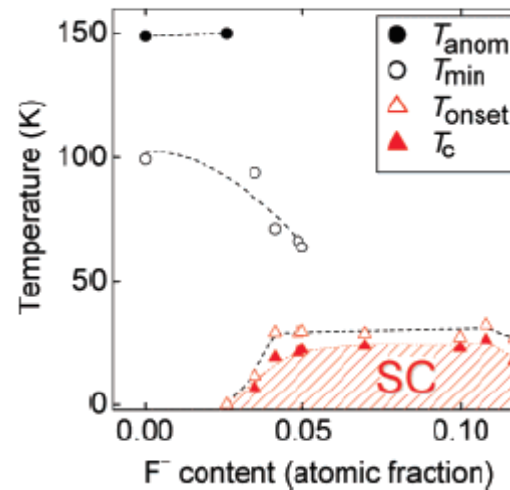
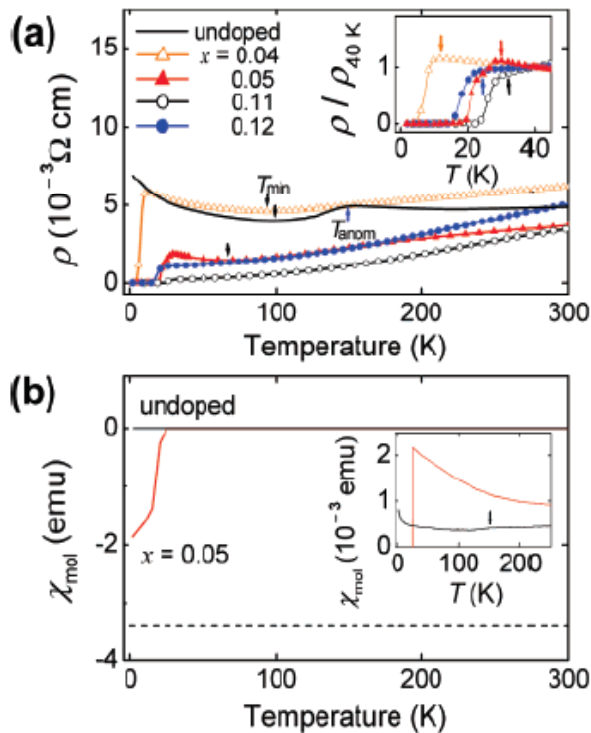
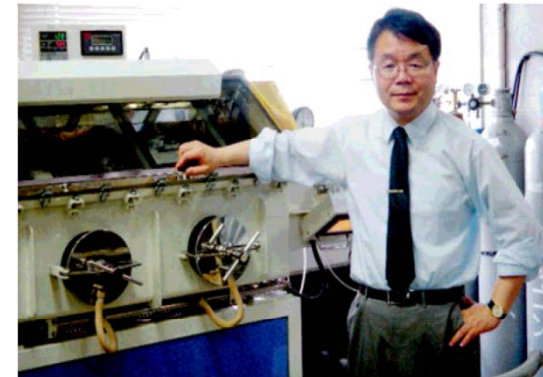
Iron-Based Layered Superconductor $\text{La}[\text{O}_{1-x}\text{F}_x]\text{FeAs}$ ($x = 0.05-0.12$) with $T_c = 26$ K

Yoichi Kamihara,^{*,†} Takumi Watanabe,[‡] Masahiro Hirano,^{†,§} and Hideo Hosono^{†,‡,§}

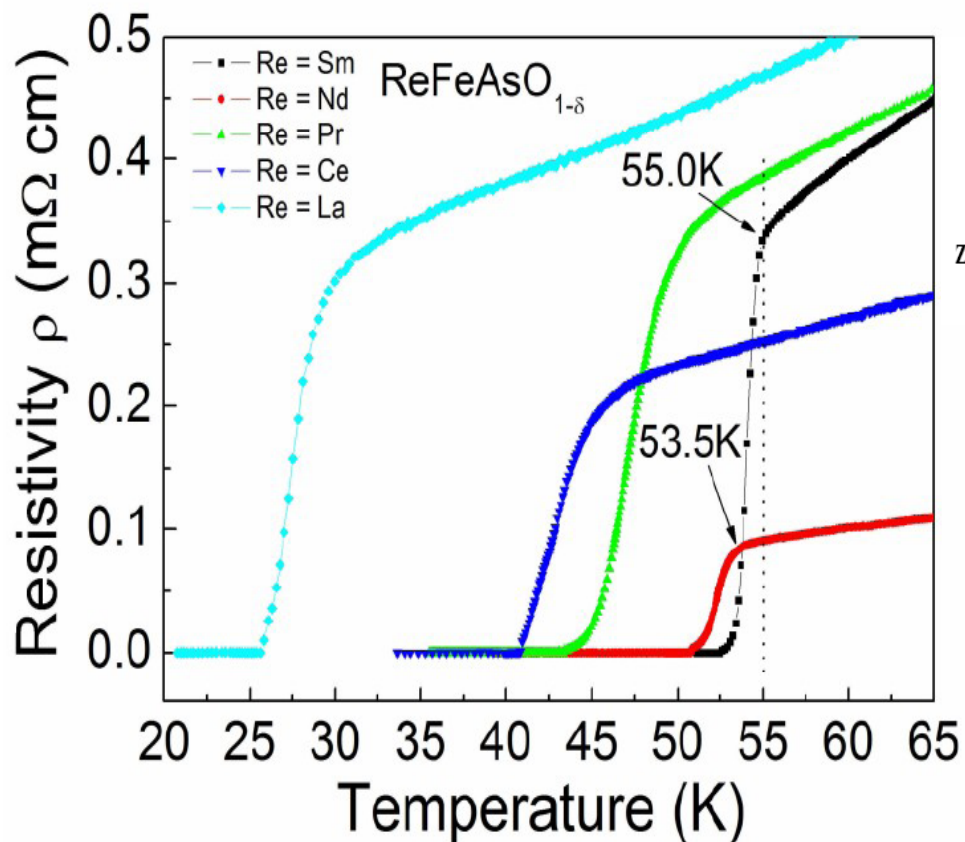
ERATO-SORST, JST, Frontier Research Center, Tokyo Institute of Technology, Mail Box S2-13, Materials and Structures Laboratory, Tokyo Institute of Technology, Mail Box R3-1, and Frontier Research Center, Tokyo Institute of Technology, Mail Box S2-13, 4259 Nagatsuta, Midori-ku, Yokohama 226-8503, Japan

Received January 9, 2008; E-mail: hosono@msl.titech.ac.jp

■ J. AM. CHEM. SOC. 2008, 130, 3296–3297



Electron doping!



Superconductivity and Phase Diagram in Iron-based Arsenic-oxides

$ReFeAsO_{1-\delta}$ (Re = rare earth metal) without Fluorine Doping

Zhi-An Ren*, Guang-Can Che, Xiao-Li Dong, Jie Yang, Wei Lu, Wei Yi, Xiao-Li Shen, Zheng-Cai Li, Li-Ling

Sun, Fang Zhou, Zhong-Xian Zhao*

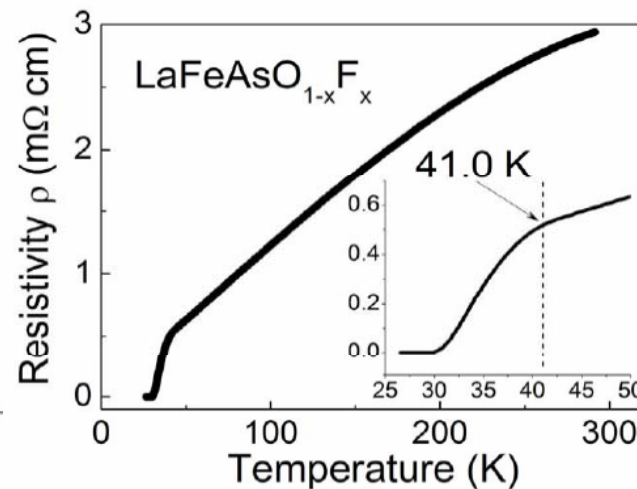
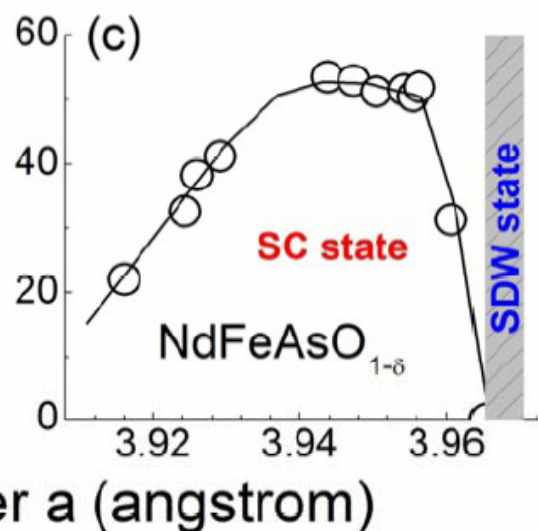
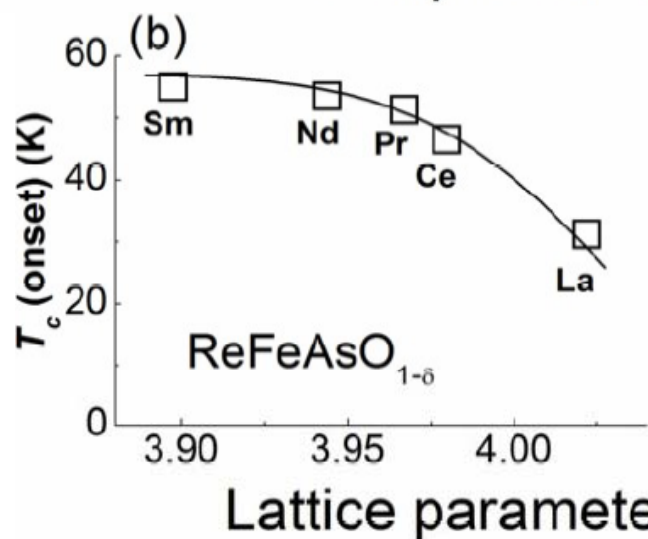
Europhysics Letters, 83 (2008)
17002

Superconductivity at 41.0 K in the F-doped $LaFeAsO_{1-x}F_x$

Wei Lu, Xiao-Li Shen, Jie Yang, Zheng-Cai Li, Wei Yi, Zhi-An Ren*, Xiao-Li Dong, Guang-Can Che, Li-Ling Sun,

Fang Zhou, Zhong-Xian Zhao*

arXiv: 0804.3725



Tc in ReOFeAs series

Table 1.

Re	a (Å)	c (Å)	T_c (onset-R) (K)	T_c (zero-R) (K)	T_c (onset-M) (K)
Sm (HP)	3.897(6)	8.407(1)	55.0	52.8	55.0
Sm (AP)	3.933(5)	8.495(3)			
Nd (HP)	3.943(7)	8.521(8)	53.5	50.9	51.0
Nd (AP)	3.965(3)	8.572(3)			
Pr (HP)	3.968(2)	8.566(1)	51.3	43.2	48.2
Pr (AP)	3.985(8)	8.600(3)			
Ce (HP)	3.979(7)	8.605(5)	46.5	41.0	42.6
Ce (AP)	3.998(1)	8.652(6)			
La (HP)	4.022(2)	8.707(1)	31.2	25.9	28.3
La (AP)	4.033(5)	8.739(1)			

Note: The HP samples are for the nominal composition of $\text{ReFeAsO}_{0.85}$, and the AP samples are for the nominal composition of ReFeAsO . And here we also note that T_c (onset) ~ 36 K in $\text{LaFeAsO}_{1.5}$ has been achieved by HP synthesis but the sample quality is still not good enough.

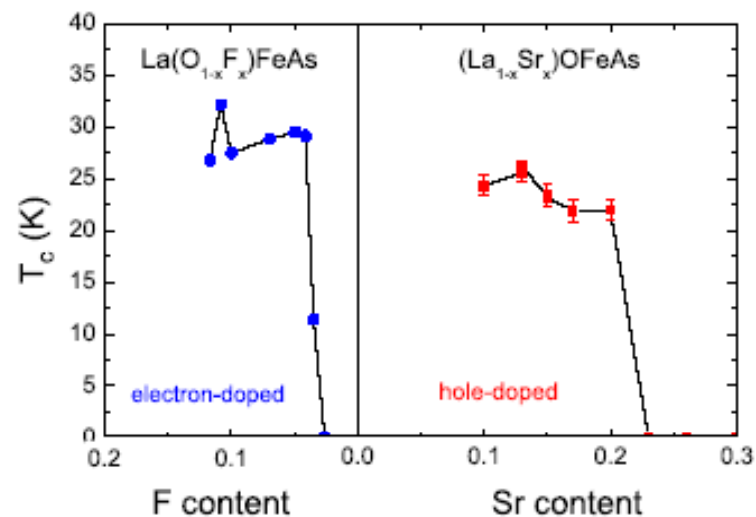
arXiv:
0804.2582

Journal of the Physical Society of Japan
Vol. 77, No. 6, June, 2008, 063707

Superconductivity at 25 K in hole doped $(\text{La}_{1-x}\text{Sr}_x)\text{OFeAs}$

HAI-HU WEN*, GANG MU, LEI FANG, HUAN YANG, and XIYU ZHU

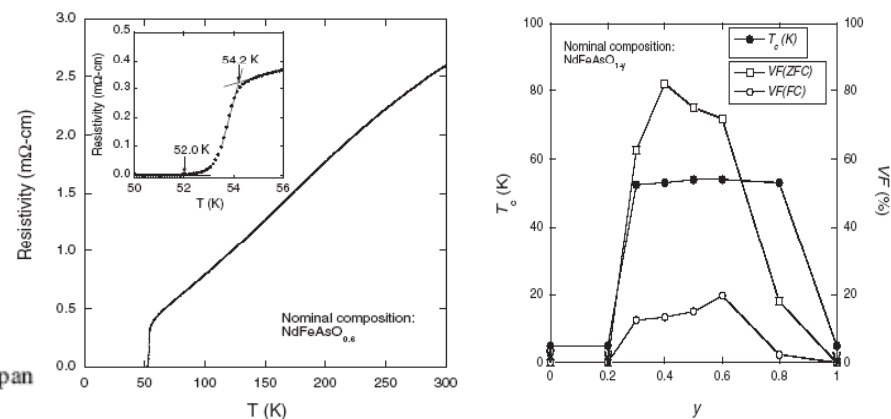
Europhys. Lett. 82, 17009 (2008)



Superconductivity at 54 K in F-Free NdFeAsO_{1-y}

Hijiri KITO, Hiroshi EISAKI, and Akira IYO*

Nanoelectronics Research Institute (NeRI), National Institute of Advanced Industrial Science and Technology (AIST), 1-1-1 Central 2, Umezono, Tsukuba, Ibaraki 305-8568

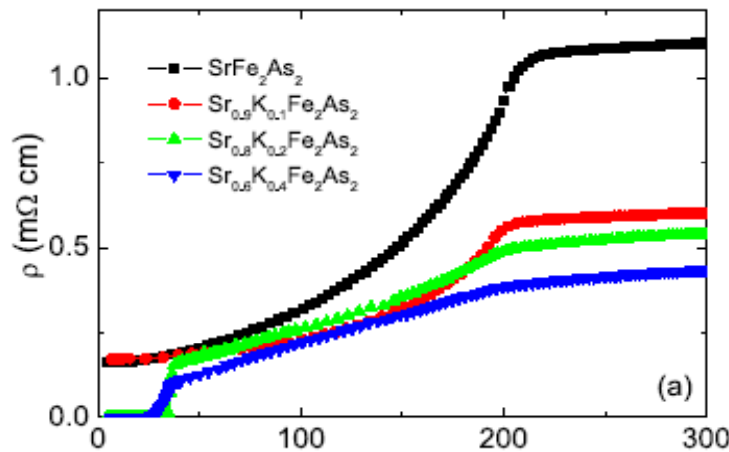
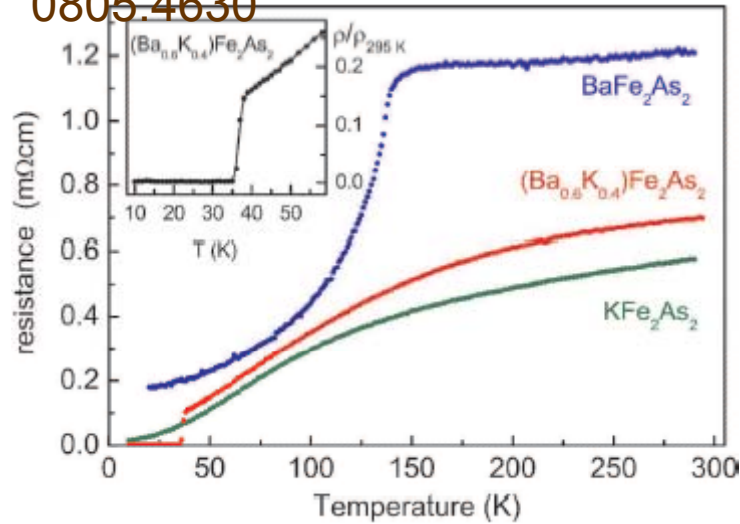


Superconductivity at 38 K in the iron arsenide $(\text{Ba}_{1-x}\text{K}_x)\text{Fe}_2\text{As}_2$

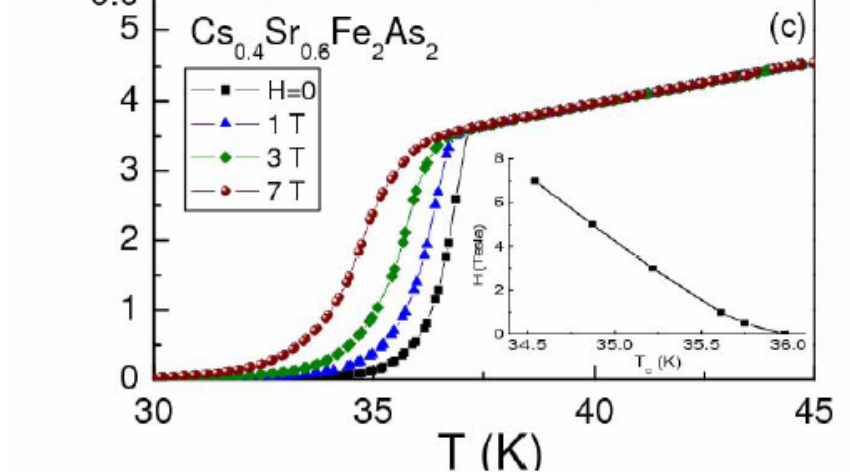
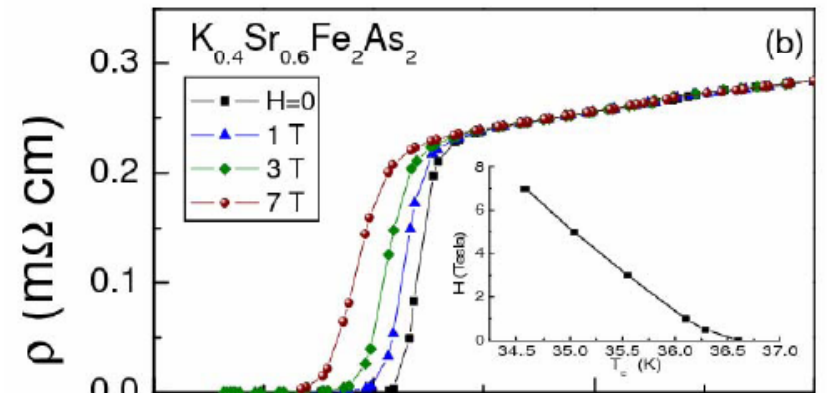
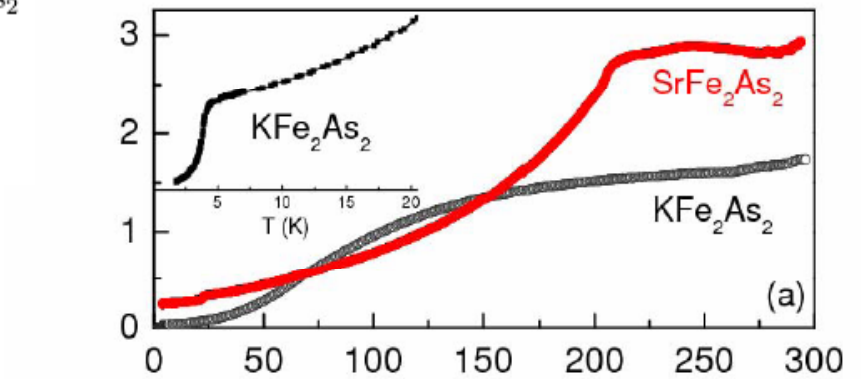
Marianne Rotter, Marcus Tegel and Dirk Johrendt*
 Department Chemie und Biochemie, Ludwig-Maximilians-Universität München,
 Butenandtstrasse 5-13 (Haus D), 81377 München, Germany
 (Dated: May 29, 2008)

arXiv:

0805.4630

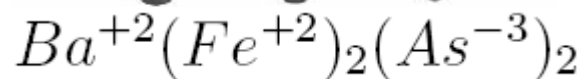
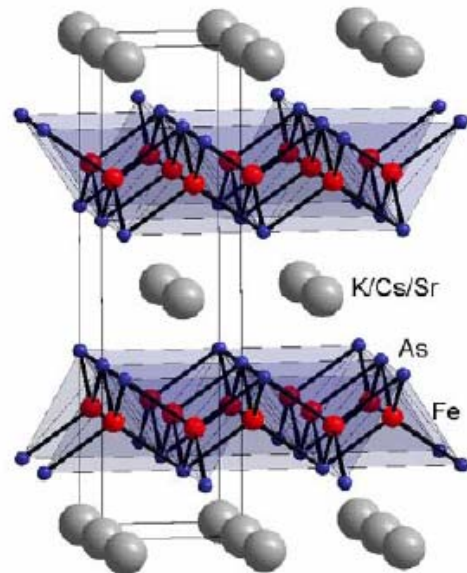
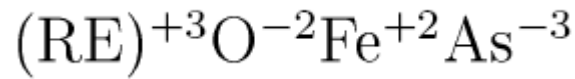
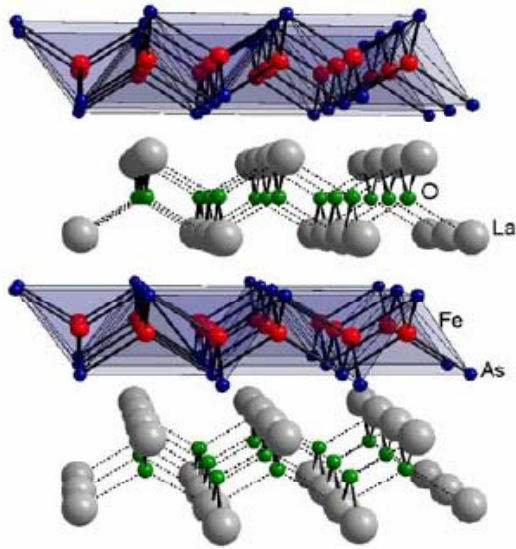


G.F.Chen et al. arXiv: 0806.1209

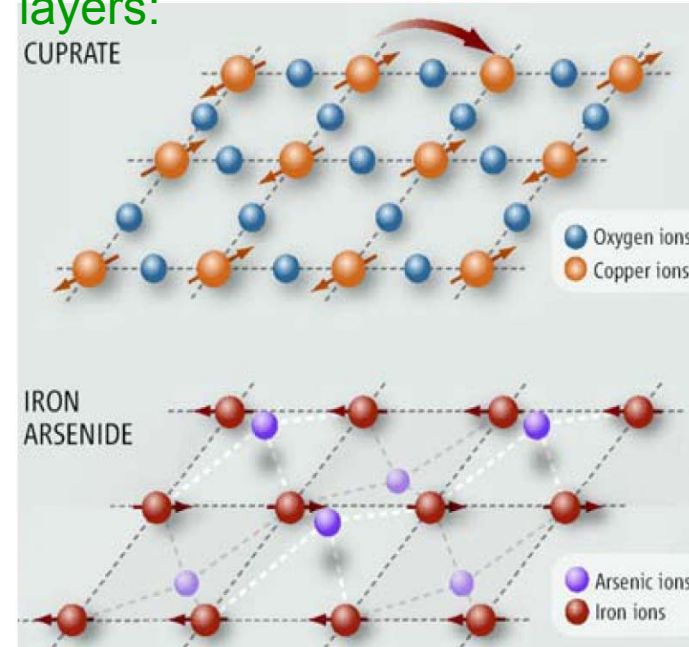


K.Sasmai et al. (C.W.Chu) arXiv: 0806.1

Basic crystal structure of FeAs superconductors

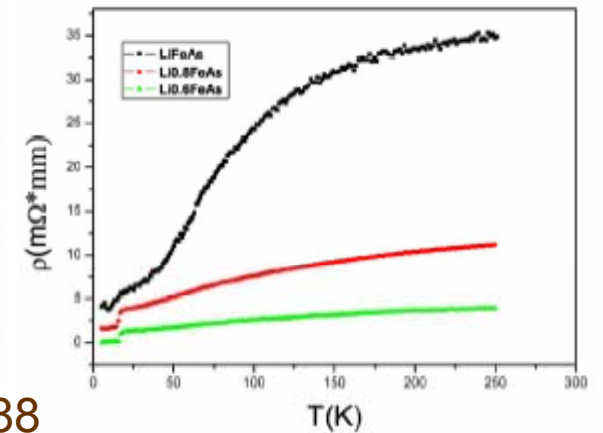
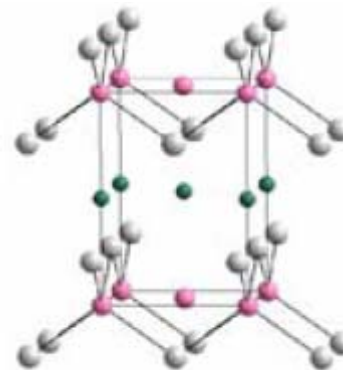


CuO₂ as compared with FeAs layers:



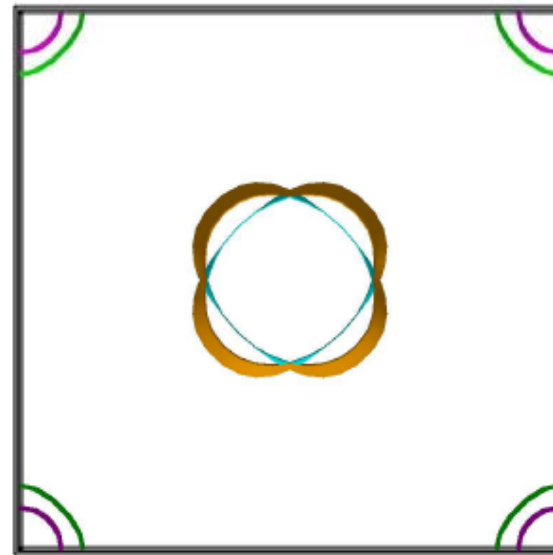
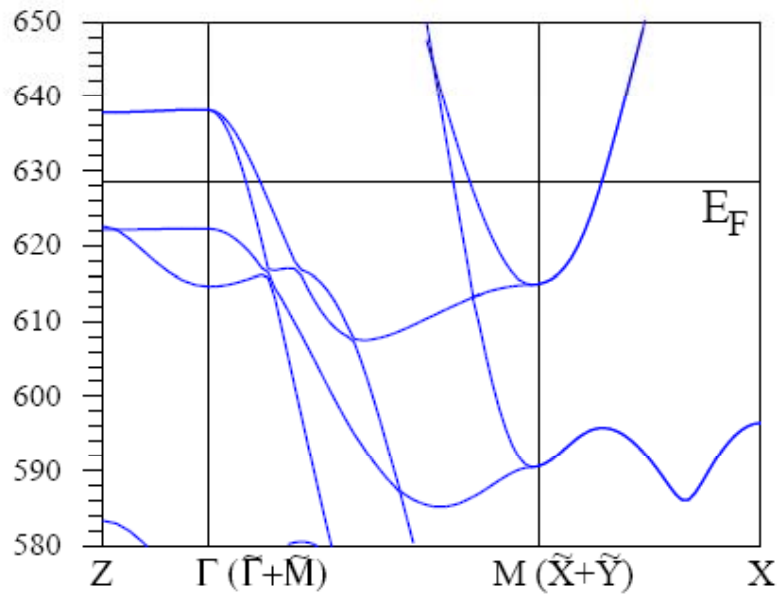
The superconductivity at 18 K in Li_{1-x}FeAs compounds

X.C.Wang, Q.Q. Liu, Y.X. Lv, W.B. Gao, L.X. Yang, R.C. Yu, F.Y. Li, C.Q. Jin*

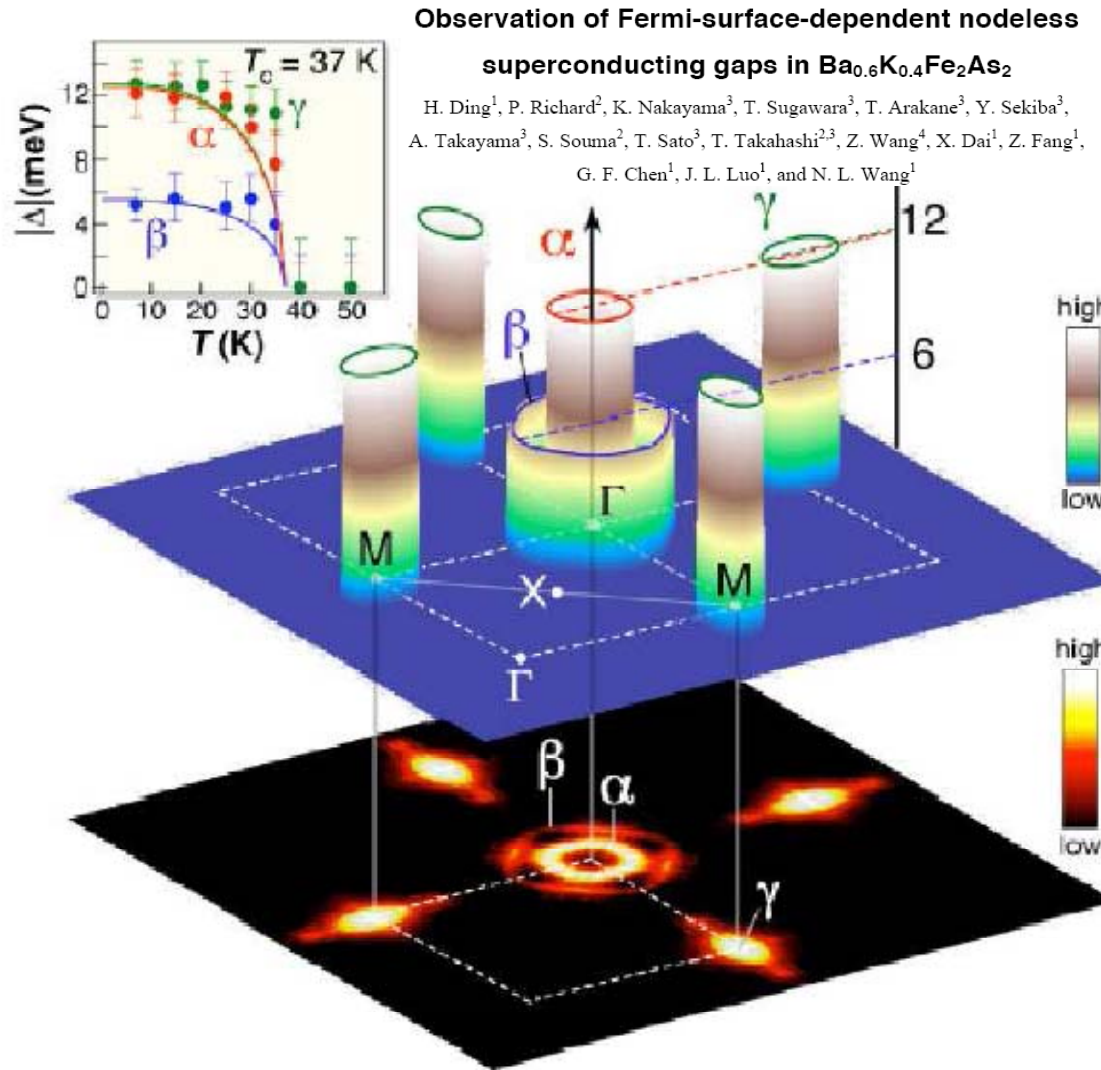


arXiv: 0806.4688

Band structure



Superconducting gap – ARPES data



arXiv: 0807.0419

Schematic picture of superconducting gaps in $\text{Ba}_{0.6}\text{K}_{0.4}\text{Fe}_2\text{As}_2$. Lower picture represents Fermi surfaces (ARPES intensity), upper insert – temperature dependence of gaps at different Sheets of the Fermi surface.

Spin fluctuations

$$\chi(\mathbf{q}, \omega) = \frac{\chi_0(\mathbf{q}, \omega)}{1 - J(\mathbf{q}, \omega) \chi_0(\mathbf{q}, \omega)}$$

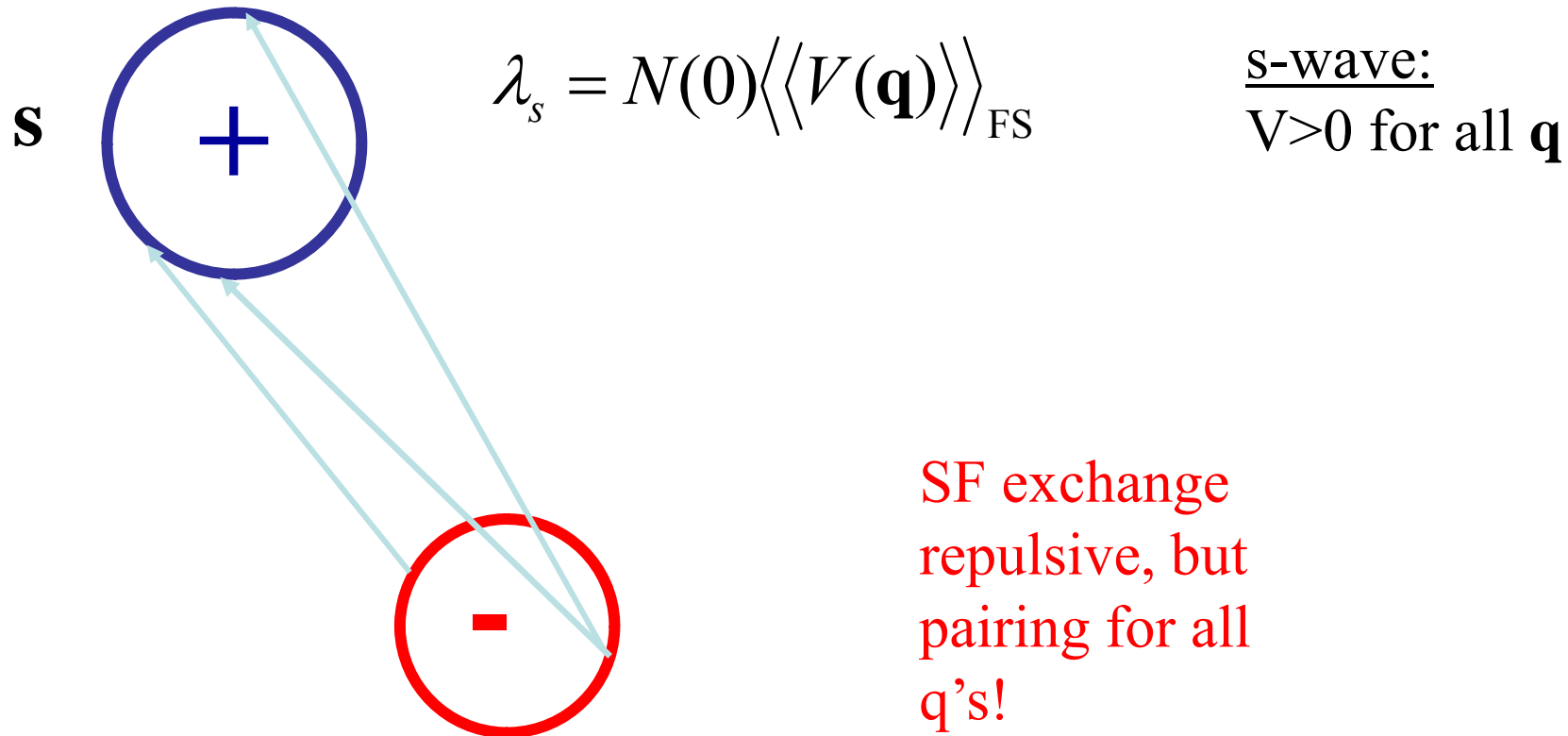
For a Mott-Hubbard system,
 $J(\mathbf{q}, \omega)$ -magnetic interaction
is *local in real space*

$$\chi_0(\mathbf{q}, \omega) = \sum_{\mathbf{k}} \frac{f(\varepsilon_{\mathbf{k}+\mathbf{q}}) - f(\varepsilon_{\mathbf{k}})}{(\varepsilon_{\mathbf{k}+\mathbf{q}} - \varepsilon_{\mathbf{k}} - \omega - i\delta)}$$

the s/c physics is just the same as old Berk-Schrieffer physics

- 1) Interaction is repulsive and peaked at $(\pi, \pi) \rightarrow$ pairing in s_{\pm} channel
- 2) Mass renormalization expected up to the energy of spin fluctuations

Repulsive pairing interactions in the $s_{+/-}$ channel:



NB: ANY magnetic interaction with this structure works in the same way, whether χ_0 -driven or J -driven, whether linear or nonlinear...

Some properties of the $s_{+/-}$ state

1. Thermodynamics is exponential in clean limit (weak coupling)
C/T, penetration depth, NMR $1/TT_1$. Singlet K
2. Reversed role of magnetic/nonmagnetic interband impurity scattering
See next slides
3. Coherence factors: depend on the probing wave vector, BCS at $q \approx 0$,
anti-BCS at $q \approx (\pi, \pi)$.
- *suppressed Hebel-Slichter peak*
suppressed Hebel-Slichter peak
4. Andreev bound states at finite energies
See next slides
5. Enhancement of spin susceptibility near $q \approx (\pi, \pi)$ below T_c
observed
7. Full gap(s) in tunneling
Full gap(s) in Andreev and in ARPES

Experiments: symmetry of the superconducting order parameter

Fully gapped superconducting state:

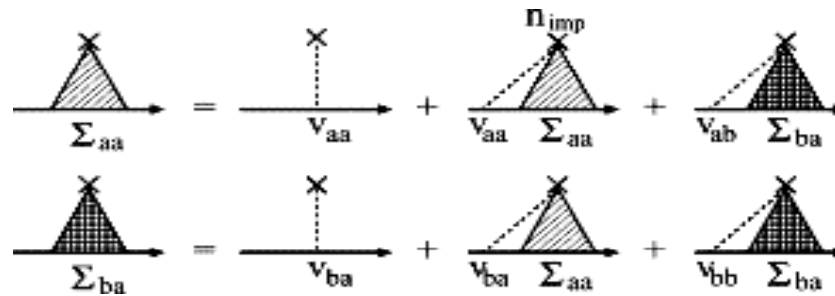
- ❑ **PCAR**: Y.Y. Chen et al., Nature 453, 1224 (2008); K.A. Yates et al., Supercond. Sci. Technol. 21, 092003 (2008); R.S. Gonnelli et al., arXiv:0807.3149.
- ❑ **ARPES**: L. Zhao et al., arXiv:0807.0398; H. Ding et al., EPL 83, 47001 (2008); T. Kondo et al., arXiv:0807.0815.
- ❑ **Penetration depth**: C. Martin et al., arXiv:0807.0876; K. Hashimoto et al., arXiv:0806.3149; L. Malone et al., arXiv:0806.3908

NMR – Lines of nodes at the FS:

- ❑ **^{75}As NMR**: $1/T_1$ with a T^3 behavior below T_c (line of nodes?)
Y. Nakai et al., JPSJ 77, 073701 (2008)
 - ❑ **^{19}F NMR**: $1/T_1$ can be explained by a two d-wave gap scenario, $\Delta = \Delta_1 + \Delta_2$, $\Delta_1 = 3.5 k_B T_c$, $\Delta_2 = 1.1 k_B T_c$
K. Matano et al., EPL 83, 57001 (2008)
-

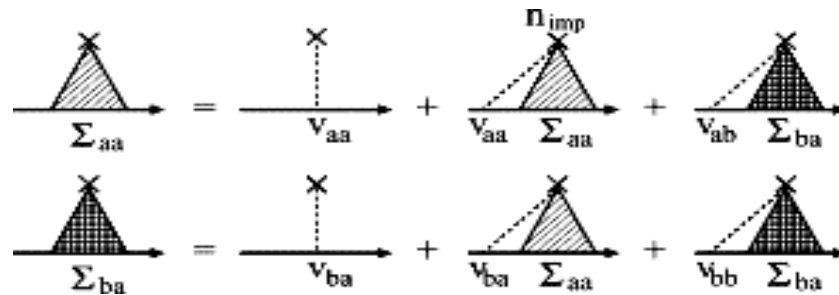
Effect of impurities

$$\hat{G} = \hat{G}_0 - \hat{\Sigma}_{imp}$$



Effect of impurities

$$\hat{G} = \hat{G}_0 - \hat{\Sigma}_{imp} \quad \hat{v} = \begin{pmatrix} 0 & v \\ v & 0 \end{pmatrix}$$



Interband impurities

$$\Sigma_{aa}^{(0)} = -i\gamma_a \frac{\sigma \bar{\omega}_{an} \sqrt{\bar{\Delta}_{bn}^2 + \bar{\omega}_{bn}^2} - (\sigma - 1) \bar{\omega}_{bn} \sqrt{\bar{\Delta}_{an}^2 + \bar{\omega}_{an}^2}}{\det a}$$

$$\Sigma_{aa}^{(1)} = \gamma_a \frac{\sigma \bar{\Delta}_{an} \sqrt{\bar{\Delta}_{bn}^2 + \bar{\omega}_{bn}^2} + (\sigma - 1) \bar{\Delta}_{bn} \sqrt{\bar{\Delta}_{an}^2 + \bar{\omega}_{an}^2}}{\det a},$$

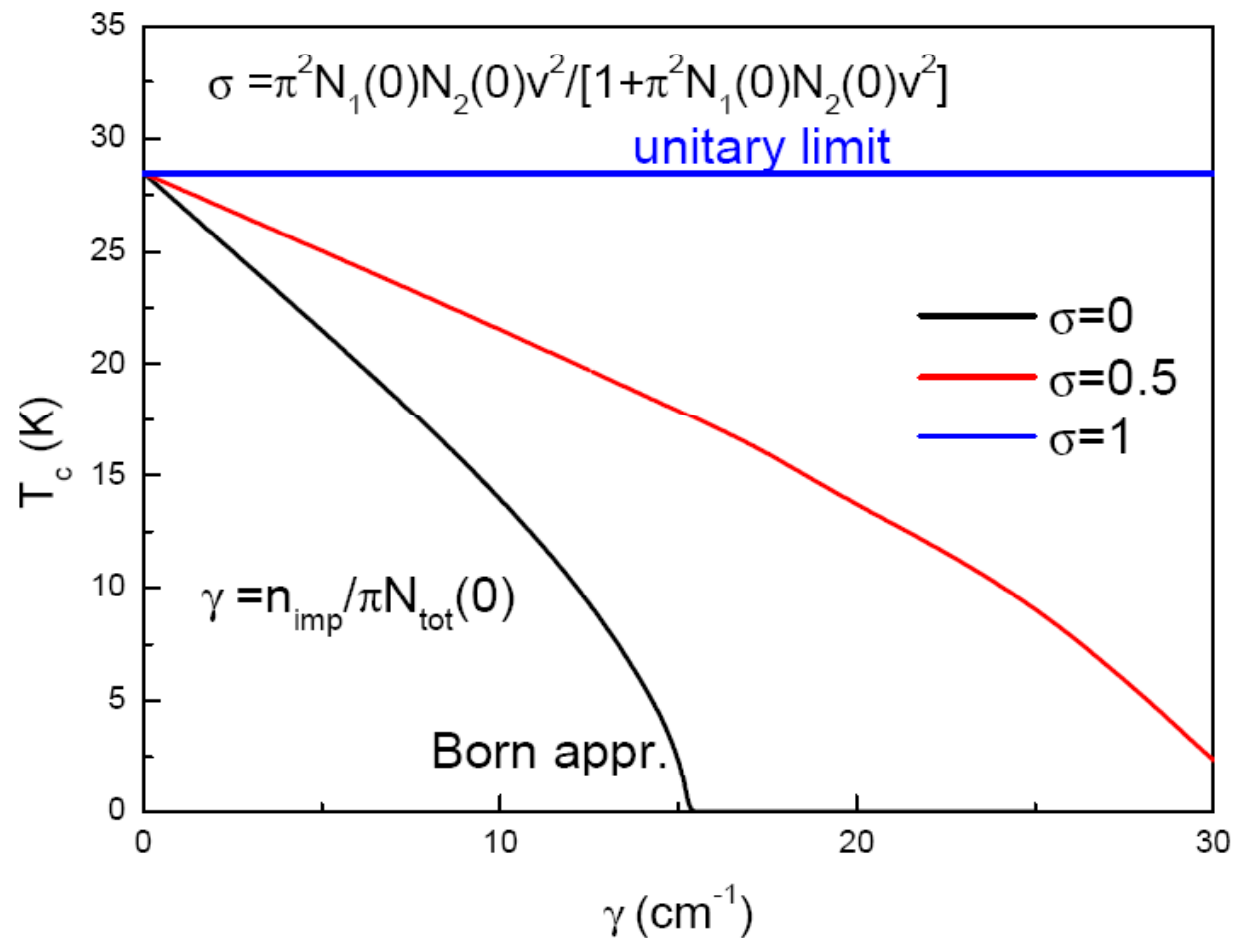
where $\gamma_i = \frac{n_{imp} \sigma}{\pi N_i(0)}$, and $\sigma = \frac{\pi^2 N_a(0) N_b(0) u^2}{1 + \pi^2 N_a(0) N_b(0) u^2}$.

$$\det a = \left[2\sigma(\sigma - 1) \left(\sqrt{\bar{\Delta}_{an}^2 + \bar{\omega}_{an}^2} \sqrt{\bar{\Delta}_{bn}^2 + \bar{\omega}_{bn}^2} - \bar{\omega}_{an} \bar{\omega}_{bn} + \bar{\Delta}_{an} \bar{\Delta}_{bn} \right) + \sqrt{\bar{\Delta}_{an}^2 + \bar{\omega}_{an}^2} \sqrt{\bar{\Delta}_{bn}^2 + \bar{\omega}_{bn}^2} \right].$$

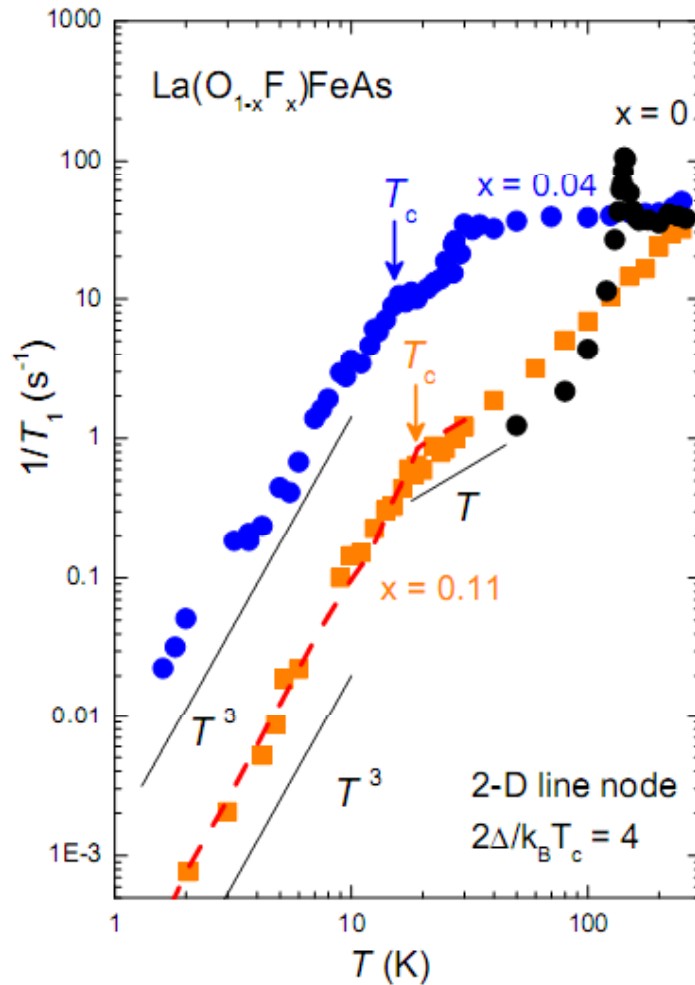
Robustness of T_c in the presence of impurities

$$\bar{\omega}_{an} = \omega_n + \gamma_{ab} \text{sign} \omega_n$$

$$\bar{\Delta}_{an} = \Delta_{an} + \gamma_{ab} \left[\sigma \bar{\Delta}_{an} / \bar{\omega}_{an} - (1 - \sigma) \bar{\Delta}_{bn} / \bar{\omega}_{bn} \right] \text{sign} \omega_n$$

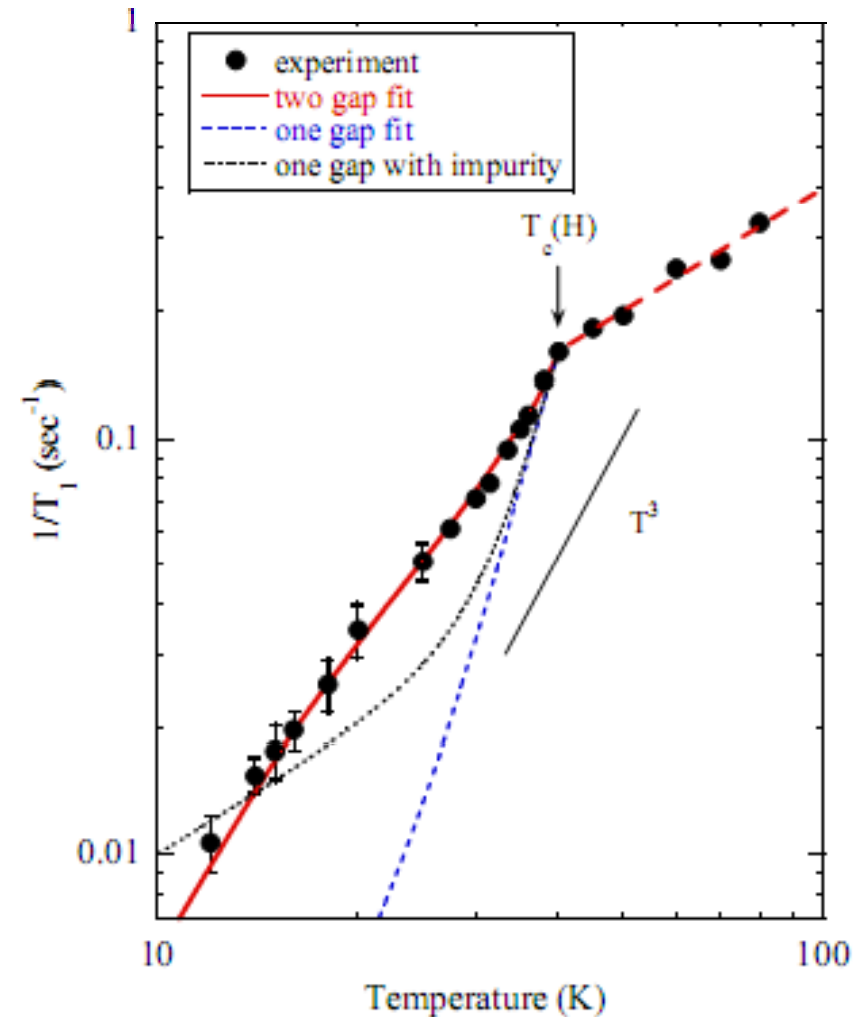


NMR experiments: superconductivity



⁷⁵As NMR: $1/T_1$ with a T^3 behavior (line of nodes?)

Y. Nakai et al., JPSJ 77, 073701 (2008)



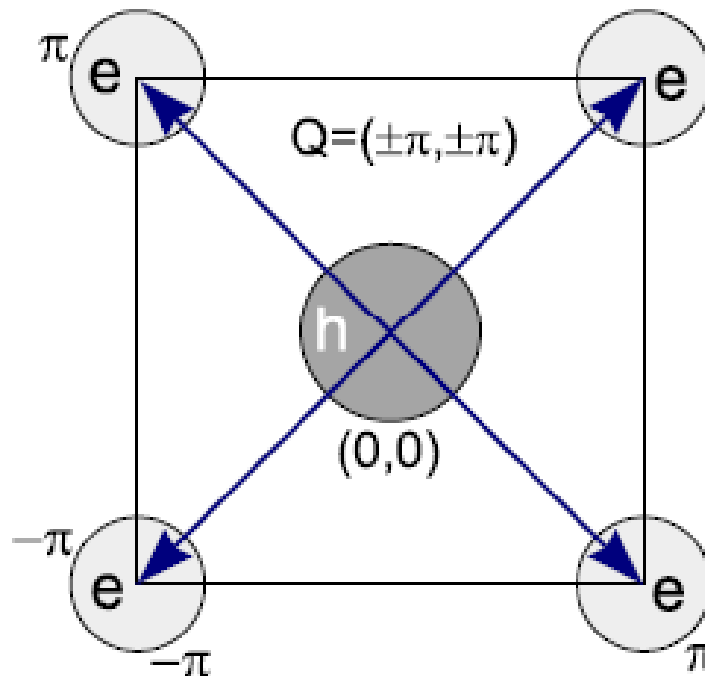
¹⁹F NMR: $1/T_1$ can be explained by a two d-wave gap scenario,
 $\Delta = \Delta_1 + \Delta_2$, $\Delta_1 = 3.5 k_B T_c$, $\Delta_2 = 1.1 k_B T_c$

K. Matano et al., EPL 83, 57001 (2008)

How to reconcile s_{\pm} model with NMR $1/T_1$?

Use simplest model

Two types of pockets (h and e) at the Fermi surface in the *folded* BZ, reproduce LDA topology



Obtain spin-lattice relaxation rate using interband susceptibility χ_{12} :

$$1/T_1 T \propto \lim_{\omega \rightarrow 0} \text{Im } \chi_{12}(\omega) / \omega$$

Absence of the Hebel-Slichter peak

Weak coupling: $\frac{1}{T_1 T} \propto \sum_{\mathbf{k}\mathbf{k}'} \left(1 + \frac{\Delta_1 \Delta_2}{E_{\mathbf{k}} E_{\mathbf{k}'}} \right) \left[-\frac{\partial f(E_{\mathbf{k}})}{\partial E_{\mathbf{k}}} \right] \delta(E_{\mathbf{k}} - E_{\mathbf{k}'})$

s-wave

$$\Delta_1 = \Delta_2 = \Delta$$

$$\frac{1}{T_1} \propto \int_{\Delta(T)}^{\infty} dE \frac{E^2 + \Delta^2}{E^2 - \Delta^2} \operatorname{sech}^2\left(\frac{E}{2T}\right)$$

Hebel-Slichter peak

Absence of the Hebel-Slichter peak

Weak coupling:
$$\frac{1}{T_1 T} \propto \sum_{\mathbf{k}\mathbf{k}'} \left(1 + \frac{\Delta_1 \Delta_2}{E_{\mathbf{k}} E_{\mathbf{k}'}} \right) \left[-\frac{\partial f(E_{\mathbf{k}})}{\partial E_{\mathbf{k}}} \right] \delta(E_{\mathbf{k}} - E_{\mathbf{k}'})$$

s-wave

$$\Delta_1 = \Delta_2 = \Delta$$

$$\frac{1}{T_1} \propto \int_{\Delta(T)}^{\infty} dE \frac{E^2 + \Delta^2}{E^2 - \Delta^2} \operatorname{sech}^2\left(\frac{E}{2T}\right)$$

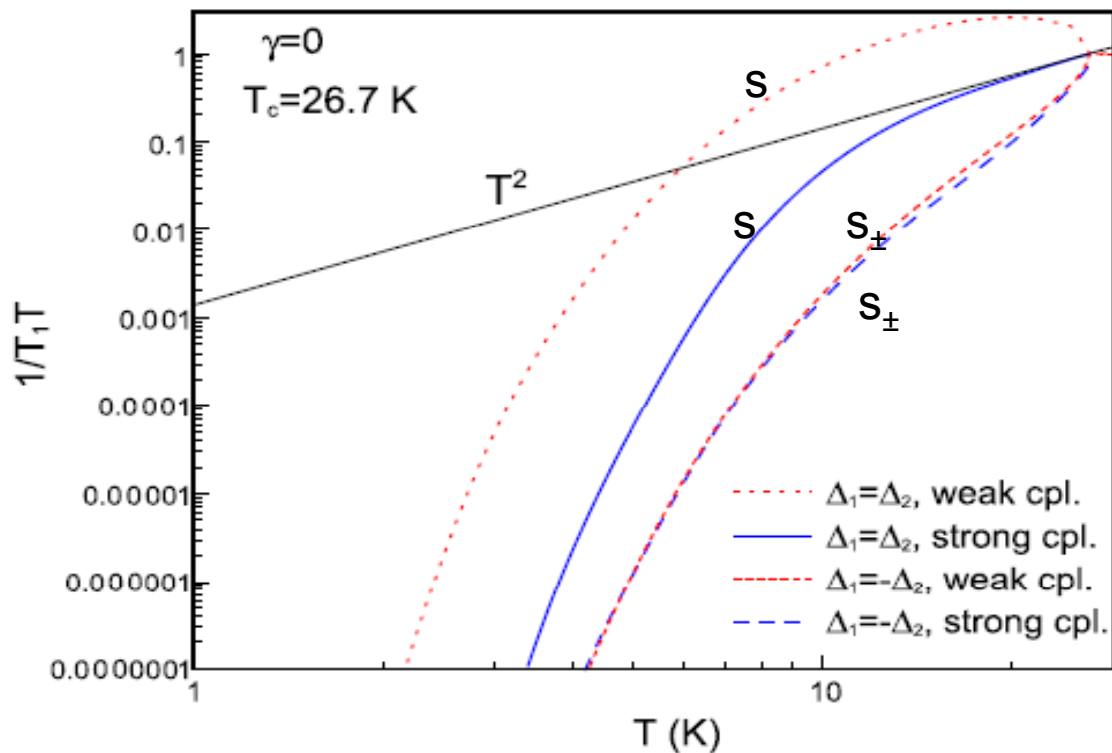
Hebel-Slichter peak

simplest s_{\pm} -wave

$$\Delta_1 = -\Delta_2 = \Delta$$

$$\frac{1}{T_1} \propto \int_{\Delta(T)}^{\infty} dE \frac{E^2 - \Delta^2}{E^2 - \Delta^2} \operatorname{sech}^2\left(\frac{E}{2T}\right) = \int_{\Delta(T)}^{\infty} dE \operatorname{sech}^2\left(\frac{E}{2T}\right)$$

No Hebel-Slichter peak!



Strong-coupling limit

$$\frac{1}{T_1 T} \propto \int_0^\infty d\omega \left(-\frac{\partial f(\omega)}{\partial \omega} \right) \{ [\text{Re}g_1^Z(\omega) + \text{Re}g_2^Z(\omega)]^2 + [\text{Re}g_1^\Delta(\omega) + \text{Re}g_2^\Delta(\omega)]^2 \}.$$

Here $g_i^Z(\omega) = n_i(\omega) Z_i(\omega) \omega / D_i(\omega)$

$g_i^\Delta(\omega) = n_i(\omega) \phi_i(\omega) / D_i(\omega)$

$D_i(\omega) = \sqrt{[Z_i(\omega)\omega]^2 - \phi_i^2(\omega)}$.

$\phi_i(\omega) = Z_i(\omega) \Delta_i(\omega)$ ← complex order parameter
Eliashberg equations:

$Z_i(\omega)$ is the mass renormalization
 $n_i(\omega)$ is a partial density of states

$$\phi_i(\omega) = \sum_j \int_{-\infty}^{\infty} dz K_{ij}^\Delta(z, \omega) \text{Re}g_j^\Delta(z) + i\gamma \frac{g_1^\Delta(\omega) - g_2^\Delta(\omega)}{2\mathcal{D}}$$

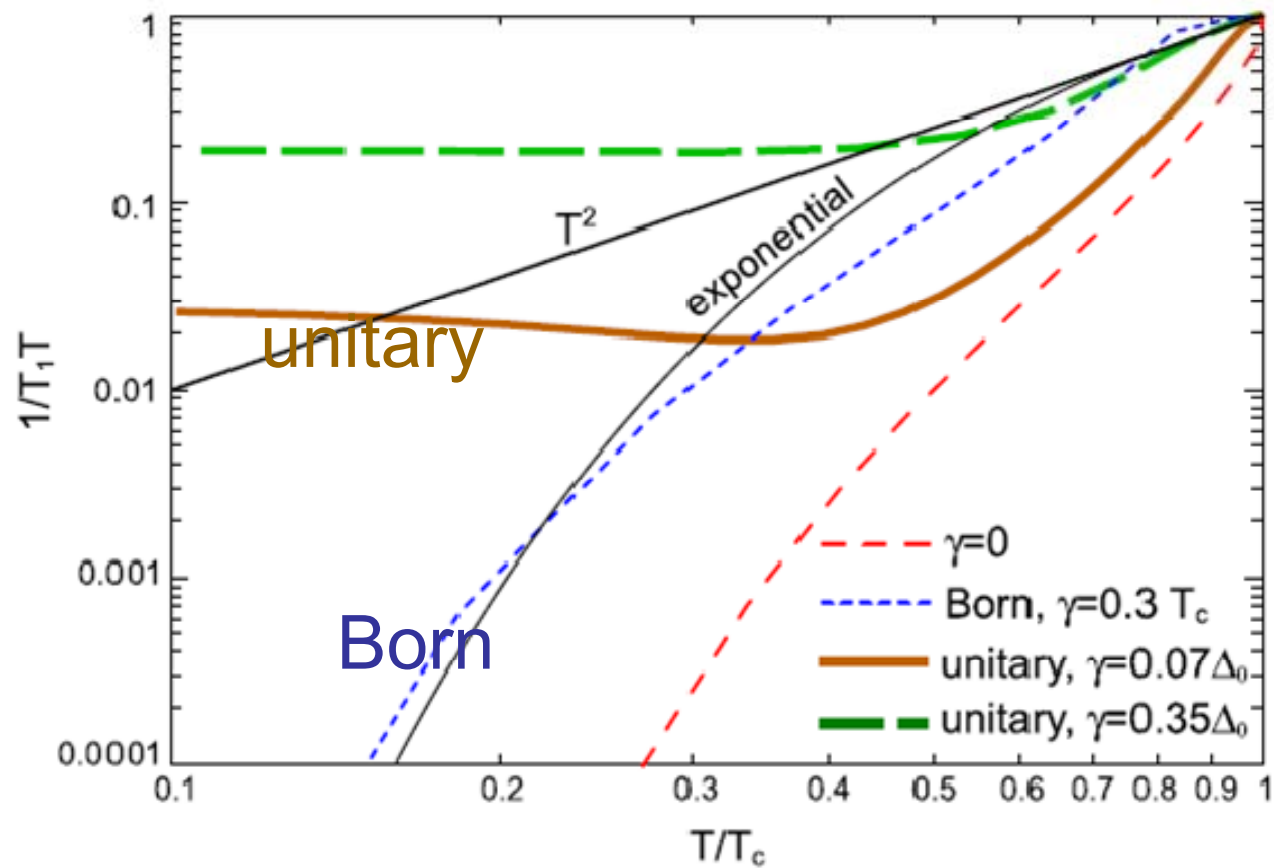
$$(Z_i(\omega) - 1)\omega = \sum_j \int_{-\infty}^{\infty} dz K_{ij}^Z(z, \omega) \text{Re}g_j^Z(z) + i\gamma \frac{g_1^Z(\omega) + g_2^Z(\omega)}{2\mathcal{D}}$$

$$\sigma = \frac{[\pi N(0)v]^2}{1 + [\pi N(0)v]^2}$$

$$\mathcal{D} = 1 - \sigma + \sigma \{ [g_1^Z(\omega) + g_2^Z(\omega)]^2 - [g_1^\Delta(\omega) - g_2^\Delta(\omega)]^2 \}$$

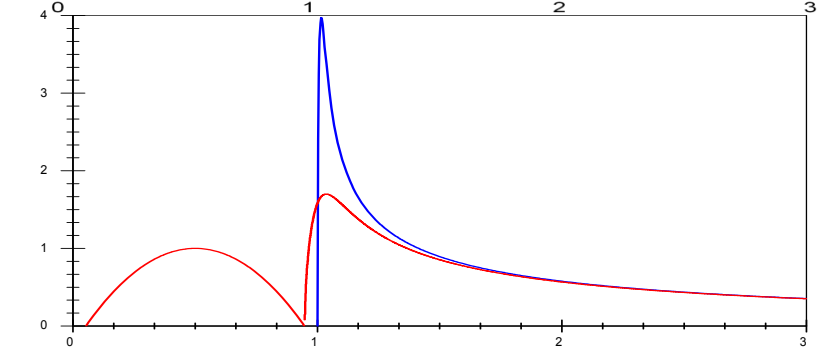
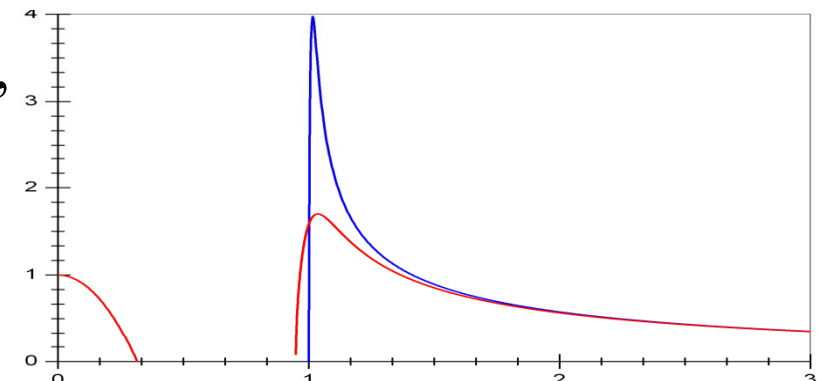
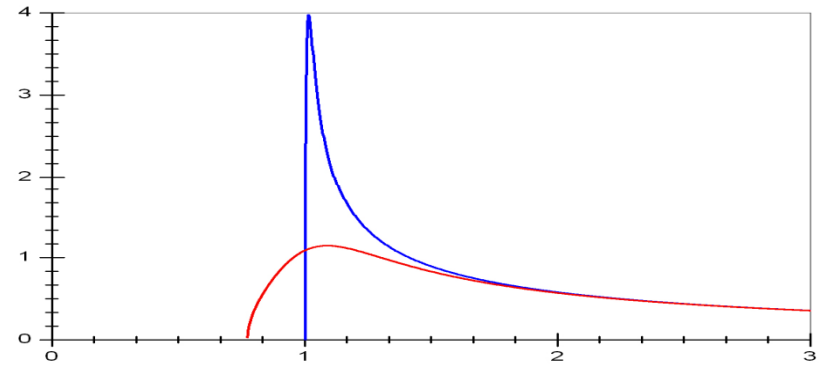
$\gamma = 2c\sigma/N(0)$ is the normal-state scattering rate,
 c is the impurity concentration, v is the impurity potential, σ is the impurity strength ($\sigma \rightarrow 0$: Born limit, $\sigma = 1$: unitary limit)

The dependence of $1/T_1$ is not reproduced in both Born and unitary limits:

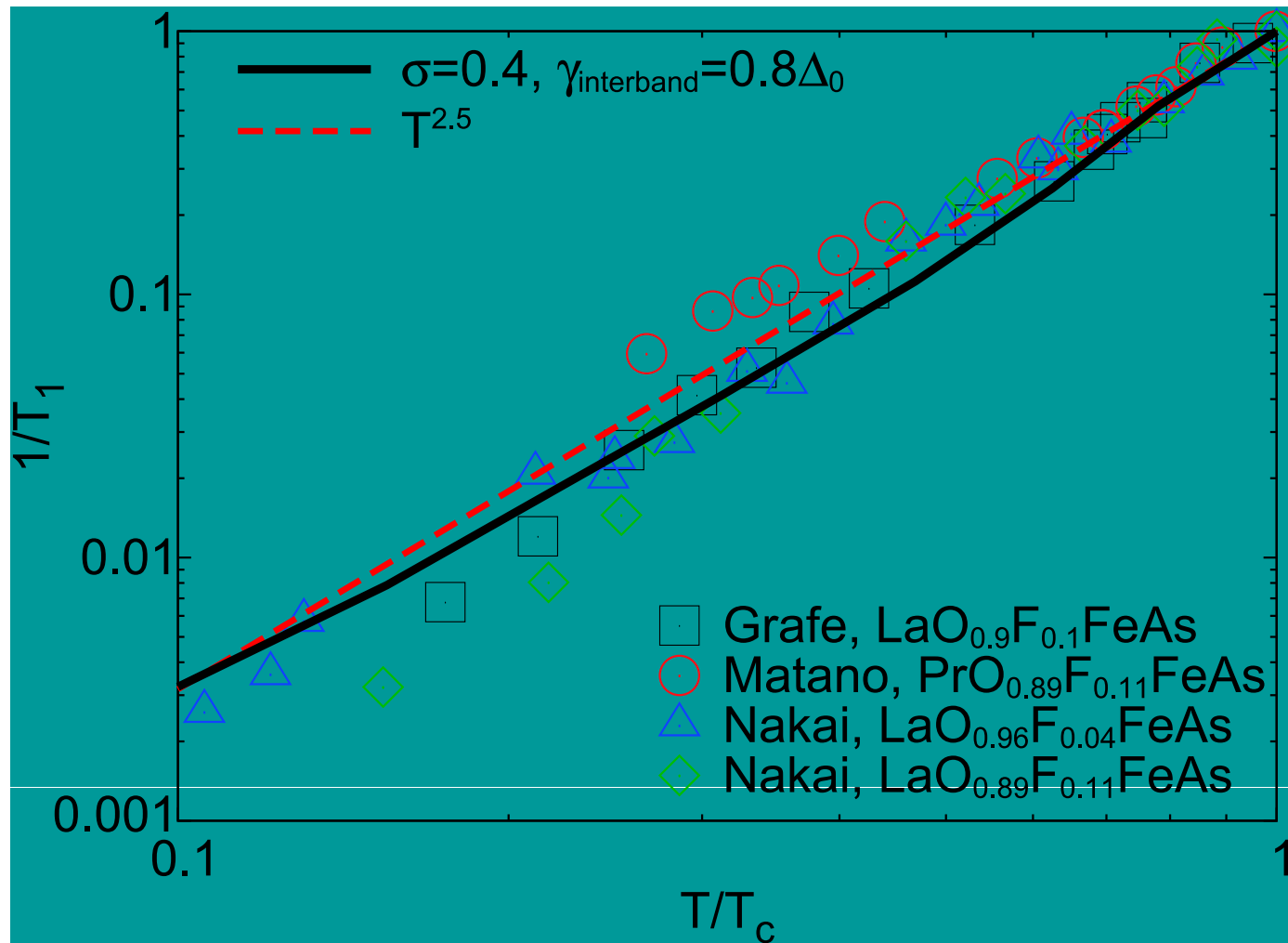


Impurity scattering: intermediate regime

1. Nonmagnetic impurities are pair breaking
2. Born limit: no coherence peak, exponential at low T
3. Unitary limit: weak T_c suppression, zero-energy bound state
4. **Intermediate limit: finite energy bound state, simulates power law**

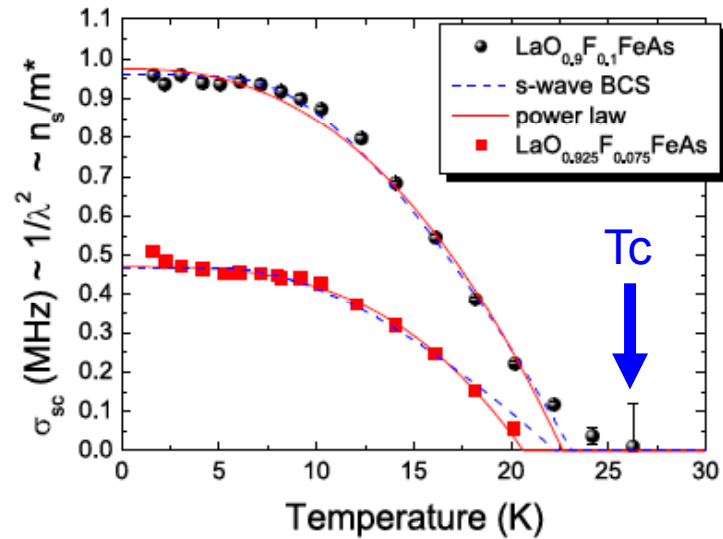


NMR: possible explanation of low-T behavior

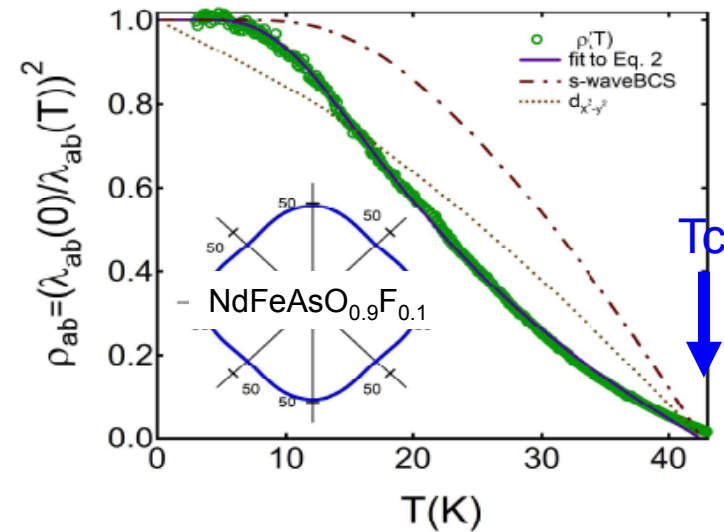


Superfluid density n_s : experiment

μ SR: Luetkens, arXiv:0804.3115



μ SR: Martin et al, arXiv:0807.0876



Superfluid density: the model

$$1/\lambda_{L,\alpha\beta}^2(T) \equiv (\omega_{p,\alpha\beta}^{sf}(T)/c)^2 = \sum_{i=\sigma,\pi} \left(\frac{\omega_{p,i}^{\alpha\beta}}{c} \right)^2 \pi T \sum_{n=-\infty}^{\infty} \frac{\tilde{\Delta}_i^2(n)}{[\tilde{\omega}_i^2(n) + \tilde{\Delta}_i^2(n)]^{3/2}}$$

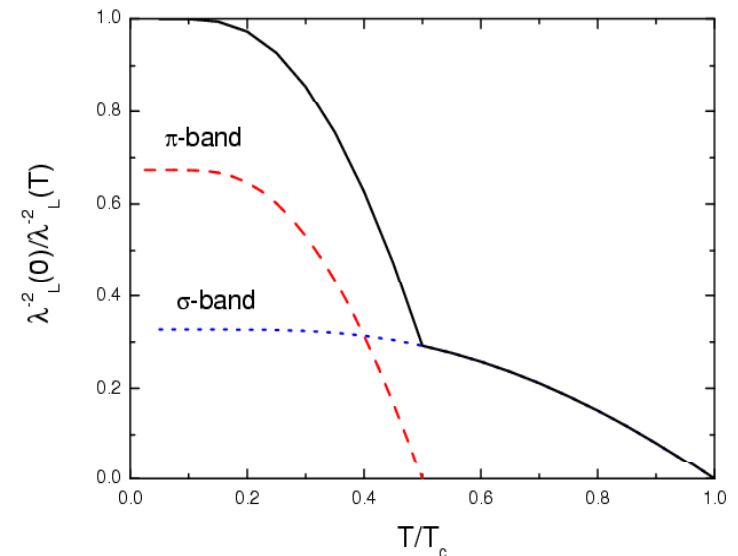
where $\tilde{\omega}(n) = \omega_n Z(\omega_n)$ and $\tilde{\Delta}(\omega_n) = \Delta(\omega_n) Z(\omega_n)$ are the solutions of the Eliashberg equations.

Effects of impurities

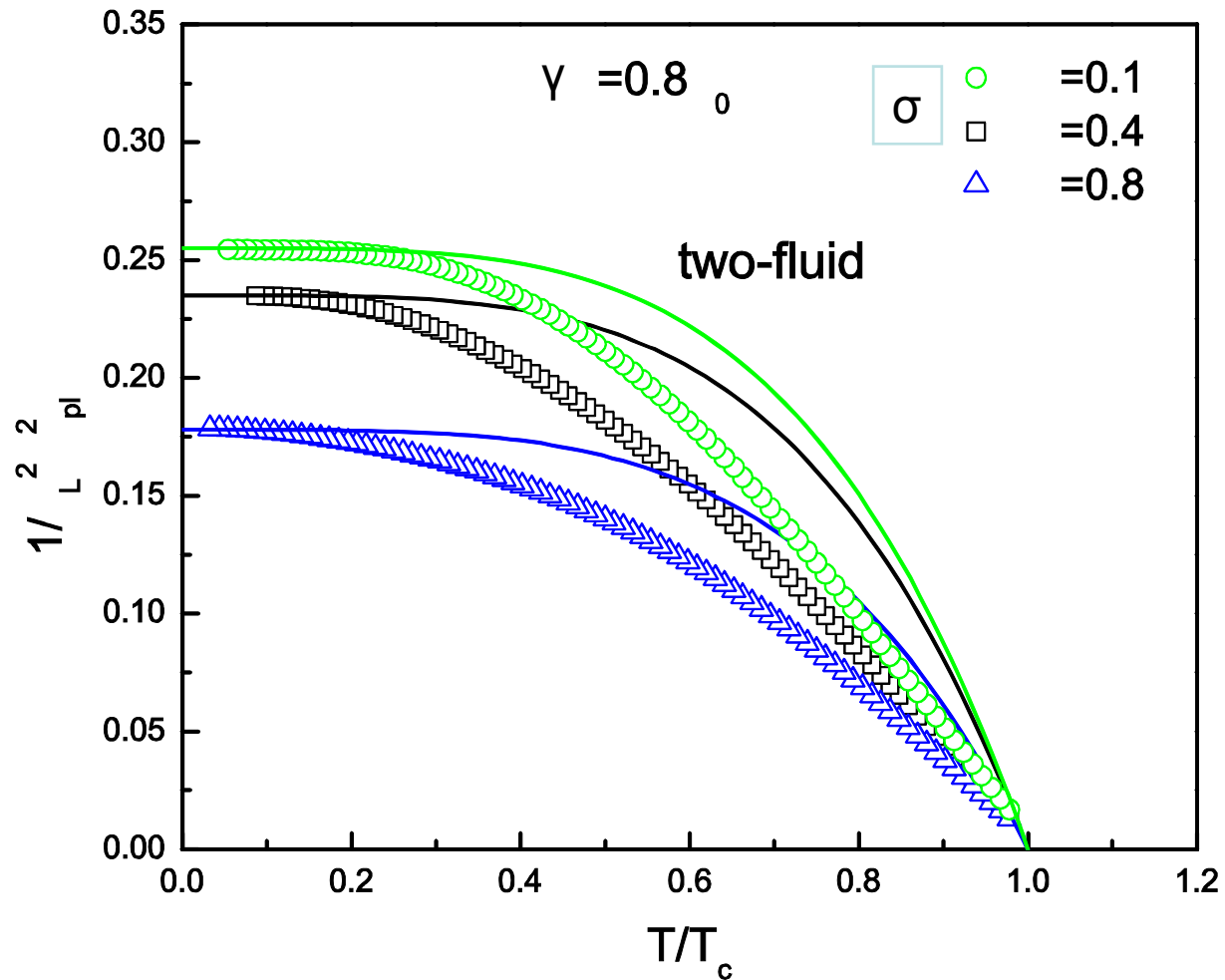
$$\Delta_i \rightarrow \Delta_i^0 + \sum_j \gamma_{ij} \Delta_j / 2 \sqrt{\omega_n^2 + \Delta_j^2},$$

$$Z(\omega_n) \rightarrow Z^0(\omega_n) + \sum_j \gamma_{ij} / 2 \sqrt{\omega_n^2 + \Delta_j^2}$$

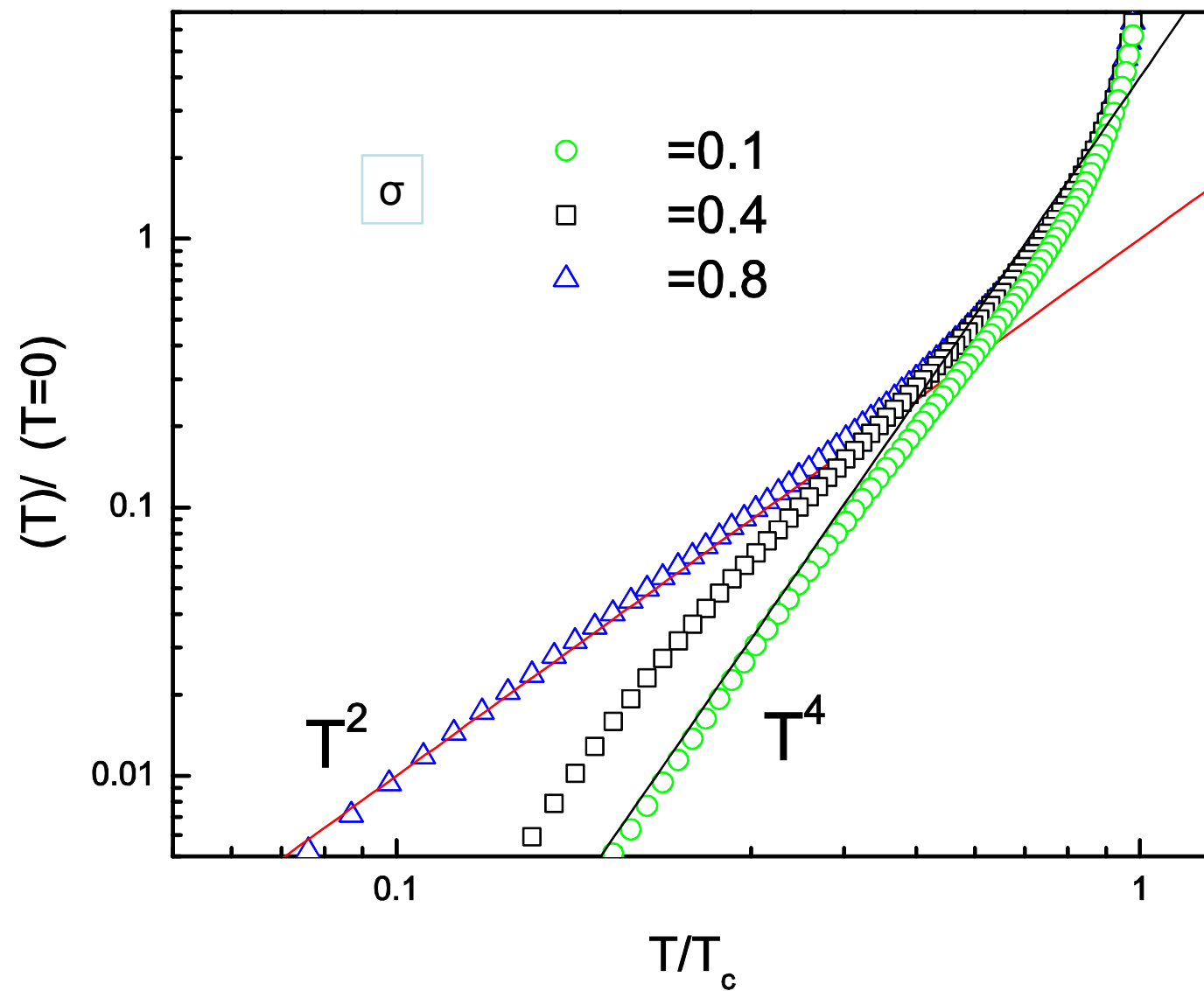
The case of weakly coupled bands (MgB2)



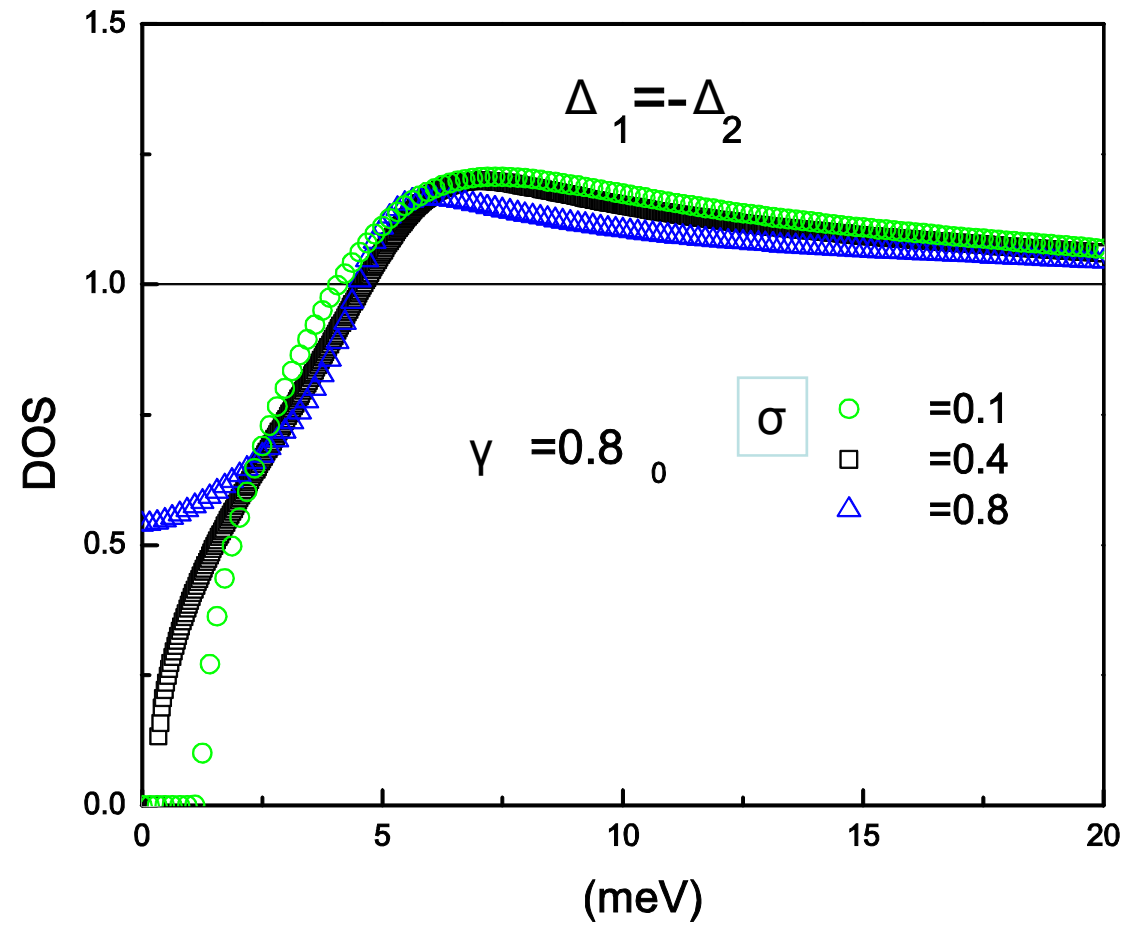
Magnetic field penetration depth



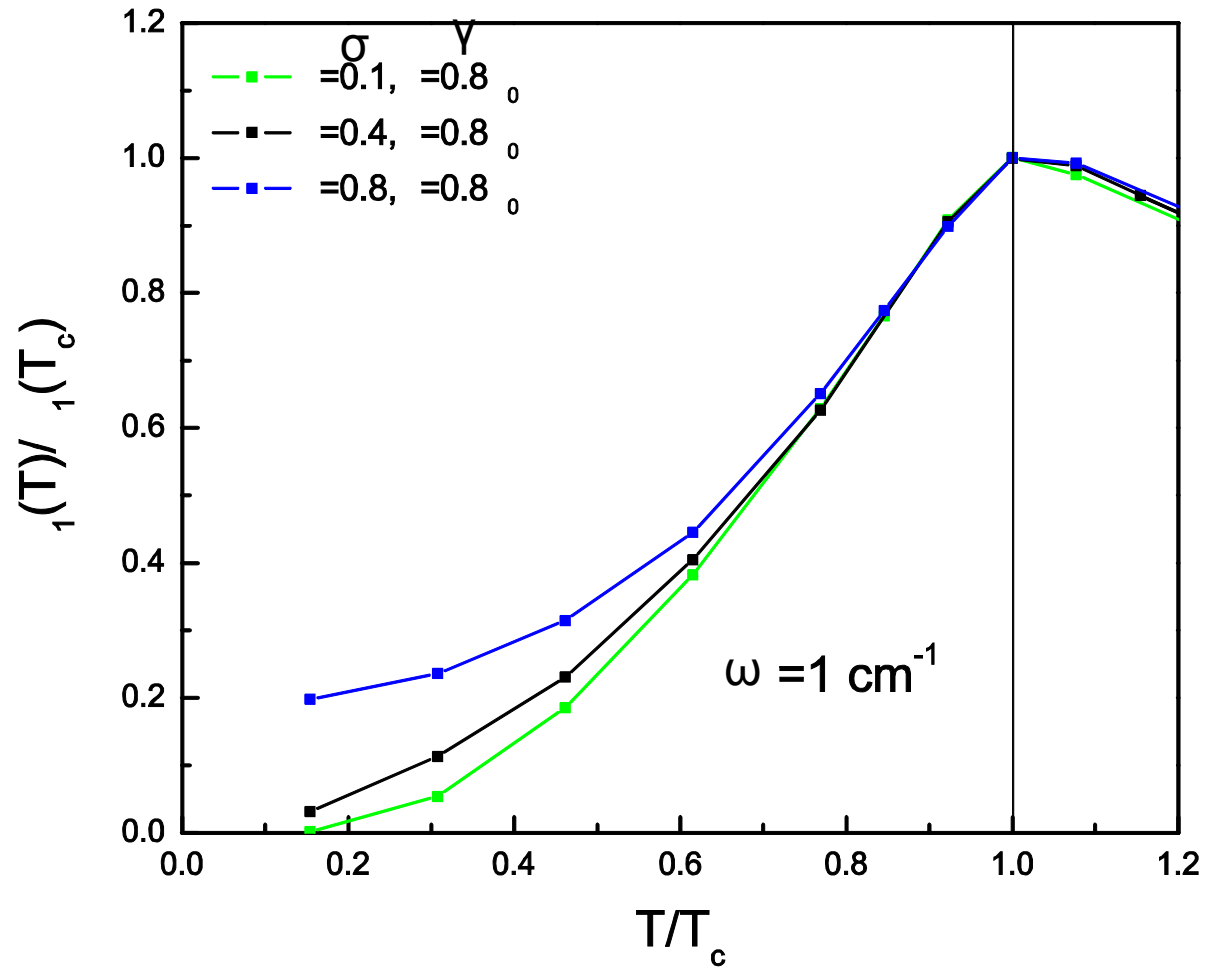
Magnetic field penetration depth: low T



Low energy density of states (DOS)



The microwave conductivity $\sigma_1(T)$



The model for tunneling in N/S junction:
 extending Andreev reflection formalism
 (the BTK model) to two bands

$$\Psi = \Psi_N \theta(-x) + \Psi_S \theta(x)$$

$$\Psi_N = \psi_k \begin{pmatrix} 1 \\ 0 \end{pmatrix} + a \psi_k \begin{pmatrix} 0 \\ 1 \end{pmatrix} + b \psi_{-k} \begin{pmatrix} 1 \\ 0 \end{pmatrix}$$

$$\Psi_S = c \left[\beta \phi_p \begin{pmatrix} u_1 \\ v_1 + e^{-i\varphi_1} \end{pmatrix} + \alpha \phi_q \begin{pmatrix} u_2 \\ v_2 + e^{-i\varphi_2} \end{pmatrix} \right]$$

$$+ d \left[\beta \phi_p \begin{pmatrix} v_1 \\ u_1 e^{-i\varphi_1} \end{pmatrix} + \alpha \phi_q \begin{pmatrix} v_2 \\ u_2 e^{-i\varphi_2} \end{pmatrix} \right].$$

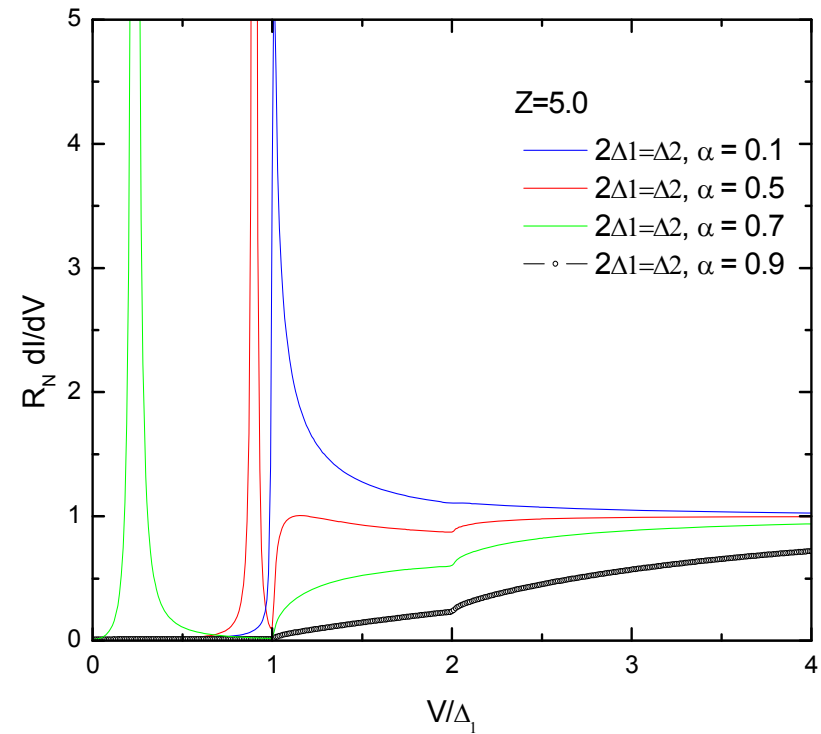
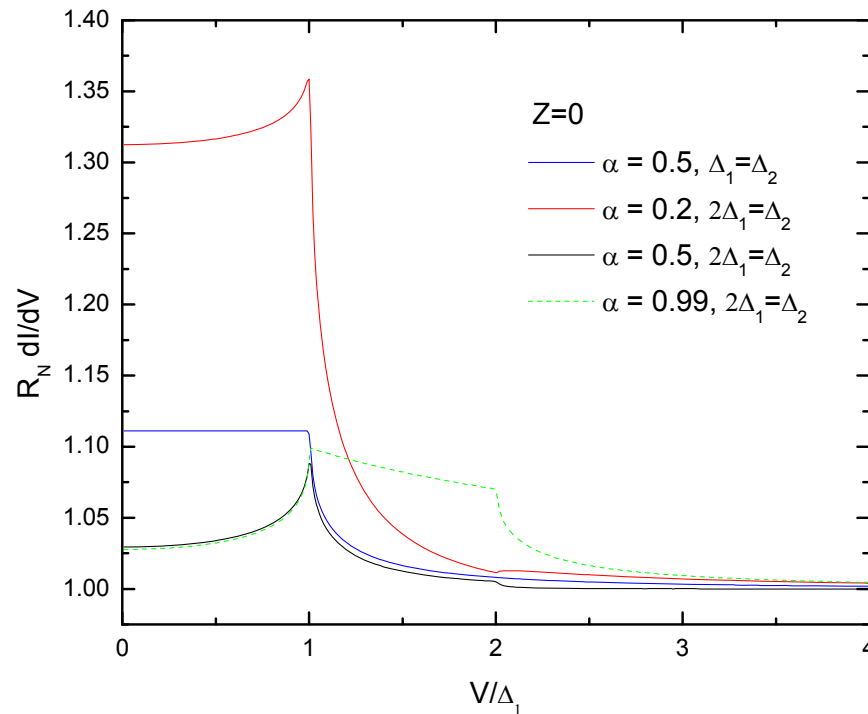
Φ_p are *Bloch functions*

and α, β are mixing coefficients between electron and hole bands

$$\alpha^2 + \beta^2 = 1$$

Tunneling conductance in the s_{\pm} case

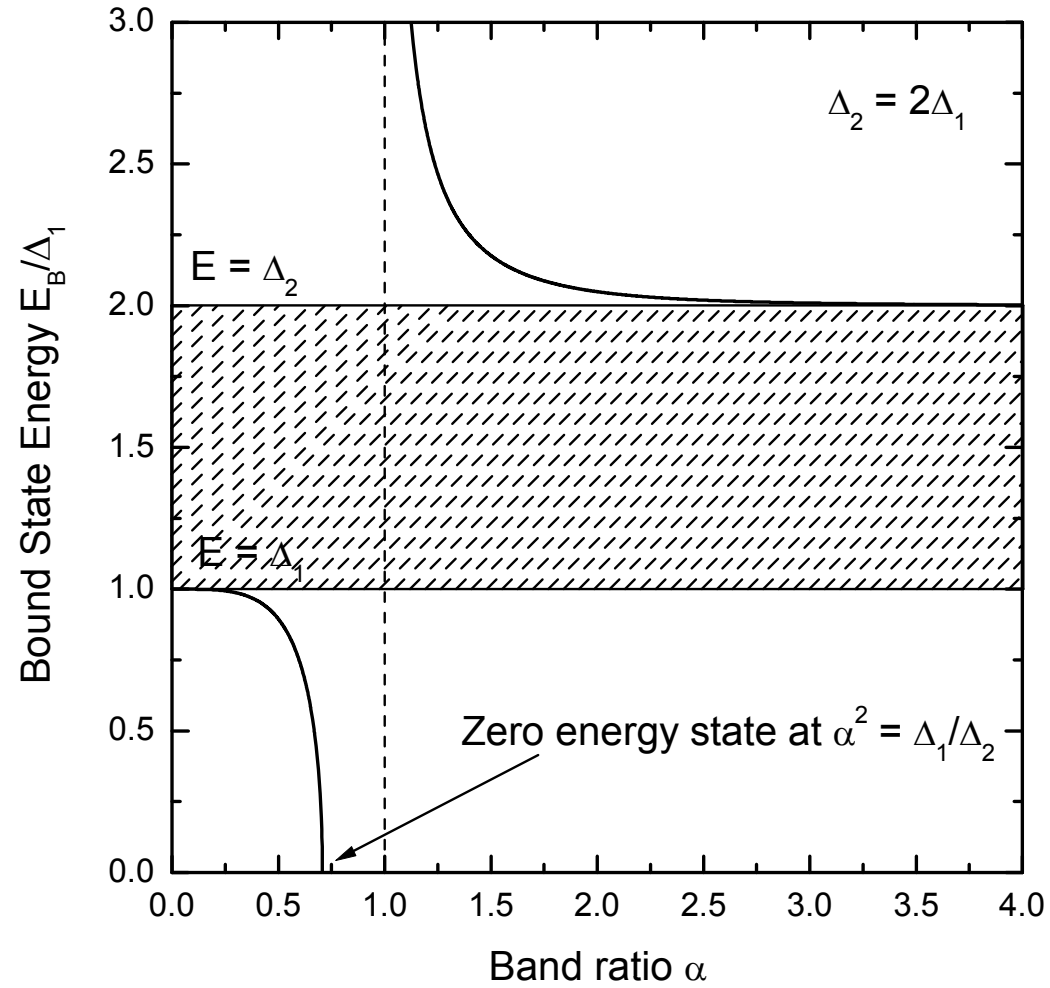
$$Z = H / \hbar v_{FN} \quad H - \text{the barrier height}$$



Andreev conductance is suppressed due to destructive **interband interference**

Bound states appear at **finite energy** for large Z

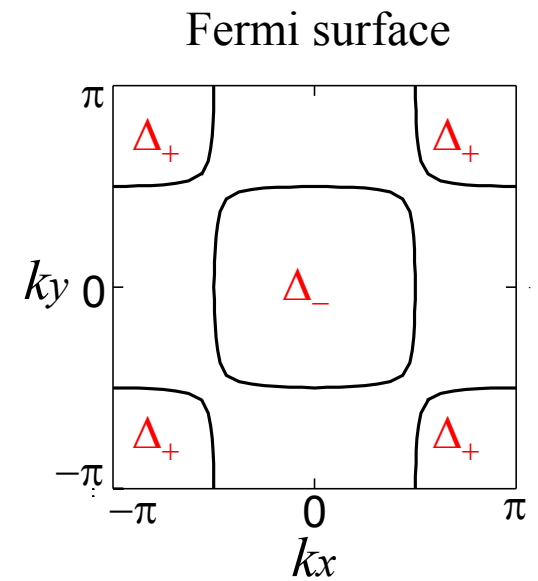
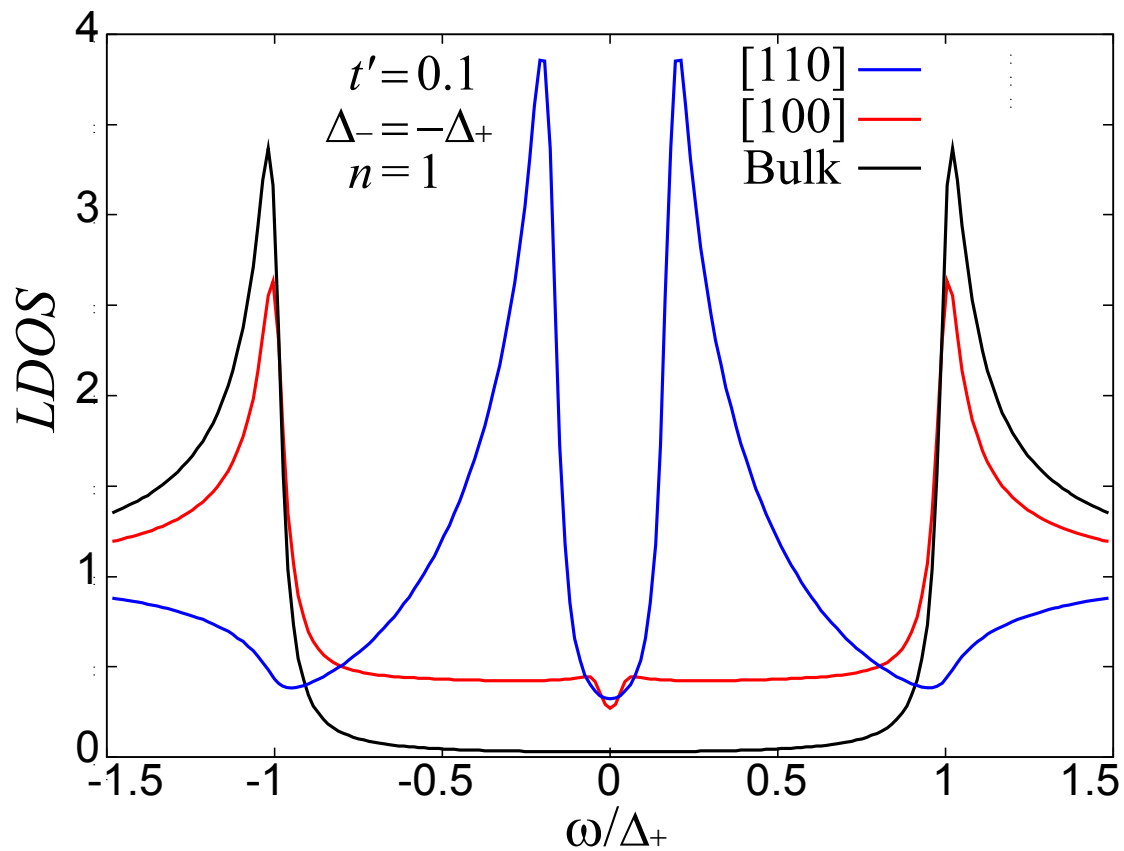
Tunneling regime: Surface bound states



LDOS at surface

$s+ -$ wave

$$\Delta_{+(-)} = +(-)0.1$$



Andreev bound state with non zero energy (Onari and Tanaka)

Conclusions

- s_{\pm} pairing can explain some properties of superconducting *Fe-pnictides*.
- T_c is robust against *unitary* interband scattering.
- The lack of an NMR Hebel-Slichter peak is fully consistent with the nodeless s_{\pm} wave symmetry of the order parameter (whether in the clean or dirty limit).
- The low-temperature power-law behavior of $1/T_1$ can be also explained in the framework of the s_{\pm} model but requires the impurity scattering beyond the Born limit.
- *Conductance Peak* can appear in *Andreev* and tunneling experiments, but, unlike nodal superconductors, at finite energy.